ELSEVIER

Thermochimica Acta 363 (2000) 23–28

thermochimica acta

www.elsevier.com/locate/tca

Solid–liquid equilibrium and thermochemical properties of organic eutectic in a monotectic system

R.N. Rai*, U.S. Rai

Department of Chemistry, Banaras Hindu University, Varanasi 221005, India

Received 1 March 2000; received in revised form 30 June 2000; accepted 2 July 2000

Abstract

The phase-diagram of an organic analogue of a metal–non-metal system, involving *p*-dichlorobenzene–succinonitrile (DCB–SCN), shows the formation of a eutectic and a monotectic with large miscibility gap in the system. The monotectic and the eutectic contain 0.0272 and 0.9429 mole fractions of SCN, respectively, and the critical temperature is 126°C above the monotectic horizontal. The heat of mixing, entropy of fusion, roughness parameter, interfacial energy and excess thermodynamic functions were calculated based on enthalpy of fusion data determined via differential scanning calorimeter method. The interfacial energy shows the applicability of wetting condition, while the microstructures of the pure components, namely, DCB and SCN show faceted and non-faceted morphology, those of the eutectic and the monotectic show peculiar characteristic features.

Keywords: Phase diagram; Monotectic; Thermochemistry; Eutectic; Microphotograph; Organic monotectic

1. Introduction

To cater the need of current civilisation, the modern science demands materials with diverse properties. In the recent past there has been an immense research interest in the chemistry of metal eutectics [1,2], monotectics [3] and intermetallic compounds [4,5] which are a potential area of investigation in metallurgy and materials science. However, low transformation temperature, ease in purification, transparency, wider choice of materials and minimised convection effects are the special features that have prompted a number of research groups [6–8] to work on some physicochemical aspects of organic eutectics, monotectics and molecular complexes. Organic systems were used initially as model system but currently these are being used in the field ranging from semiconductors [9] to superconductors [10] as well as nonlinear optical materials [11,12]. Further, binary organic materials are known to exhibit better optical properties than their parent components.

Because of limited choice of materials and experimental difficulties associated with the miscibility gap, less attention has been focused to monotectic alloys. However, the last decade has witnessed several papers [13–15] which explain various interesting phenomena of monotectic alloys. The role of wetting behaviour, interfacial energy, thermal conductivity and buoyancy in a phase separation process has been the subject of great discussion. Seeing on the promising properties by binary organic materials we have chosen succinonitrile (SCN), a material of low entropy of fusion, simulates the metallic solidification and *p*-dichlorobenzene (DCB), a material of high entropy of fusion,

* Corresponding author. Present address: Materials Research Centre, Indian Institute of Science, Bangalore 560012, India.
E-mail address: rnrai@mrc.iisc.ernet.in (R.N. Rai).

0040-6031/00/$ – see front matter
PII: S0040-6031(00)00625-0

simulates the non-metallic solidification. As such DCB–SCN system we might say as a suitable analogue of metal–non-metal systems like Al–Si and Al–Bi. In the present paper the details studied concerning phase diagram, thermochemistry and microstructure of DCB–SCN system are discussed.

2. Experimental

2.1. Materials and purification

SCN obtained from Aldrich, Germany was purified by repeated distillation under reduced pressure. On the other hand DCB (Aldrich, Germany) was used as received. The purity of each compound was checked by comparing its melting temperature to the literature value. The melting temperature of DCB and SCN was found to be 53.5 and 56.5°C, whereas it has reported in literature 54.0 and 56°C, respectively.

2.2. Phase diagram

The phase diagram of DCB–SCN system was established in the form of temperature–composition curve. In this method mixtures of two components, under study, covering the entire range of compositions were prepared. The melting temperatures of each composition were recorded using a melting point apparatus attached with a precision thermometer associated with an accuracy of ±0.5°C.

2.3. Enthalpy of fusion

The heat of fusion of pure components, eutectic and monotectic was determined via differential scanning calorimeter (DSC) (Mettler DSC-4000 system). Indium sample was used to calibrate the system, and amount of test sample and heating rate were about 5 mg and 5 K min^{-1}, respectively, for each estimation. The values of enthalpy of fusion are reproducible within ±1.0%.

2.4. Microstructure

Microstructures of pure components, eutectic and monotectic were recorded by placing a drop of molten compound on a hot glass slide. To cover the melt, a coverslip was glided over the melt and it was allowed to cool to get a supercooled liquid. The melt was nucleated with a seed crystal of the same composition and care was taken to have unidirectional freezing. The slide with the solid was then placed on the platform of a Leitz Laborlux-D optical microscope. Different regions were viewed with suitable magnifications and photographed.

3. Results and discussion

3.1. Phase diagram

The schematic phase diagram of DCB–SCN system (Fig. 1), expressed in terms of composition and temperature, clearly shows the formation of a monotectic (0.0272 mole fraction of SCN) and a eutectic (0.9429 mole fraction of SCN), the upper consolute temperature being 126°C above the monotectic horizontal. The two components are miscible in all proportions above a critical temperature (T_c). The monotectic [3,13] is another important three phases reaction of eutectic class, which isothermally decomposes into a

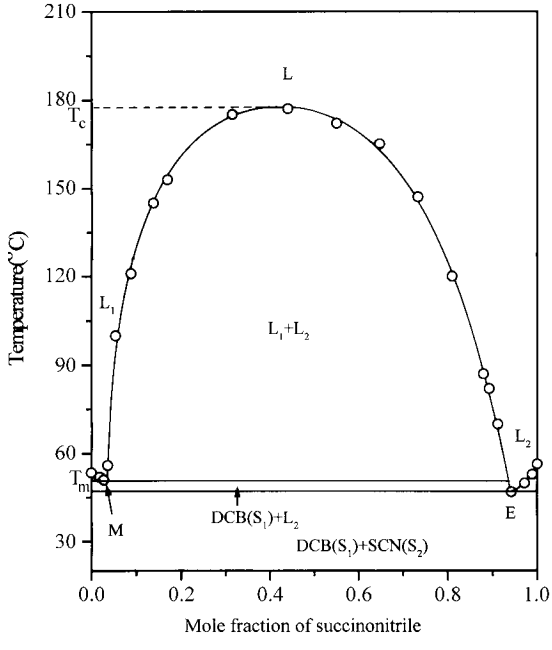

Fig. 1. Phase diagram of DCB–SCN system. (○) Melting temperature.

solid phase and another liquid phase. There are three reactions of interest on solidification of the present system. The first reaction concerns phase separation, as the liquid is cooled below the critical temperature, and can be written as

$$L \rightarrow L_1 + L_2$$

The second reaction, known as monotectic reaction, occurs when a liquid of monotectic composition (C_m) is cooled through the monotectic horizontal (T_m). In this reaction a liquid L_1 decomposes in a solid phase S_1 (rich in DCB) and another liquid phase L_2 (rich in SCN) is as follows:

$$L_1 \rightarrow S_1 + L_2$$

The third reaction that is common in phase diagrams is the eutectic reaction. On cooling the liquid of eutectic composition below the eutectic temperature, it decomposes to give two solids S_1 (rich in DCB) and S_2 (rich in SCN) as

$$L_2 \rightarrow S_1 + S_2$$

The monotectic reaction is very similar to the eutectic reaction except that one of the product phases is a second liquid phase. The monotectic, eutectic and critical solution temperatures in the present case are 51.0, 46.0 and 126.0°C, respectively.

4. Thermochemistry

4.1. Enthalpy of fusion

The idea about phase transformation, microstructure, structure of eutectic melt and nature of interaction between two components forming the eutectic and the monotectic could be obtained from a knowledge of their heat of fusion data. The experimental values of enthalpy of fusion, determined by the DSC method, are reported in Table 1. For the purpose of comparison, the value of enthalpy of fusion of eutectic calculated by the mixture law [16] is also tabulated in the same table. For the eutectic the enthalpy of mixing ($\Delta_{mix}H$) which is the difference between the experimental and the calculated values of heat of fusion is -0.08 kJ mol^{-1}. Thermochemical studies [17] suggest that the structure of a binary eutectic melt depends on the sign and magnitude of the heat of mixing. As such, three types of structures are suggested; quasi-eutectic for $\Delta_{mix}H > 0$, clustering of molecules for $\Delta_{mix}H < 0$ and molecular solution for $\Delta_{mix}H = 0$. The negative value of $\Delta_{mix}H$ for the eutectic suggests clustering of molecules in the binary melt. The entropy of fusion ($\Delta_{fus}S$) values, calculated by dividing the enthalpy of fusion by the absolute temperature corresponding to the melting point of different materials (Table 1) being positive suggest that the entropy factor, in all cases, favour the melting process.

4.2. Size of critical nucleus and interfacial energy

When a melt is cooled below its melting temperature, the liquid phase does not solidify spontaneously. This is because of the fact that below equilibrium temperature the melt contains large number of clusters of molecules of different sizes. So long as the clusters are all below the critical size [18], they cannot grow to form crystals and so no solid is formed. The critical size (r^*) of nucleus is related to interfacial energy (σ)

Table 1
Heat of fusion, entropy of fusion and roughness parameter

Materials	Heat of fusion (kJ mol^{-1})	Entropy of fusion (J mol^{-1} K^{-1})	Roughness parameter (α)
DCB	18.3	56.1	6.8
SCN	3.7	11.2	1.4
DCB–SCN monotectic			
Experimental	17.5	54.0	6.5
By mixture law	17.9		
DCB–SCN eutectic			
Experimental	4.46	14.0	1.7
By mixture law	4.54		

Table 2
Interfacial energy of DCB, SCN and their eutectic and monotectic

Parameter	Interfacial energy (mN m^{-1})
σ_{SL_2} (SCN)	9.6
σ_{SL_1} (DCB)	39.7
$\sigma_{L_1L_2}$ (DCB–SCN)	9.0
σ_E (DCB–SCN)	10.8

by the equation

$$r^* = \frac{2\sigma T_{fus}}{\Delta_{fus}H\,\Delta T} \tag{1}$$

where T_{fus}, $\Delta_{fus}H$ and ΔT are melting temperature, heat of fusion, and degree of undercooling, respectively. An estimate of the interfacial energy is given by the expression

$$\sigma = \frac{C\,\Delta_{fus}H}{(N_A)^{1/3}(V_m)^{2/3}} \tag{2}$$

where N_A is the Avogadro number, V_m the molar volume, and parameter C lies between 0.30 and 0.35. The calculated values of interfacial energy for different materials are reported in Table 2.

4.3. Excess thermodynamic functions

The deviation from the ideal behaviour can best be expressed in terms of excess thermodynamic functions which give a more quantitative idea about the nature of molecular interactions. To know the nature of interaction between two components forming eutectics, some thermodynamic functions such as excess free energy (g^E), excess enthalpy (h^E), and excess entropy (s^E) were calculated using the following equations and the values are given in Table 3:

$$g^E = RT\left[x_1 \ln \gamma_1^1 + x_2 \ln \gamma_2^1\right] \tag{3}$$

$$h^E = -RT^2\left[x_1 \frac{\partial \ln \gamma_1^1}{\partial T} + x_2 \frac{\partial \ln \gamma_2^1}{\partial T}\right] \tag{4}$$

Table 3
Excess thermodynamic functions for the eutectic

Material	g^E (kJ mol^{-1})	h^E (kJ mol^{-1})	s^E (J mol^{-1} K^{-1})
DCB–SCN eutectic	0.45	1.98	4.83

$$s^E = -R\left[x_1 \ln \gamma_1^1 + x_2 \ln \gamma_2^1 + x_1 T \frac{\partial \ln \gamma_1^1}{\partial T} + x_2 T \frac{\partial \ln \gamma_2^1}{\partial T}\right] \tag{5}$$

It is evident from Eqs. (3)–(5) that activity coefficient and its variation with temperature are required to calculate the excess functions. Activity coefficient (γ^1) could be evaluated [16,19] by using the equation

$$-\ln(x_i^1 \gamma_i^1) = \frac{\Delta_{fus}H_i}{R}\left(\frac{1}{T_{fus}} - \frac{1}{T_i}\right) \tag{6}$$

where x_i^1, $\Delta_{fus}H_i$, T_i and T_{fus} are mole fraction, enthalpy of fusion, melting temperature of component i and eutectic temperature, respectively. The variation of activity coefficient with temperature could be calculated by differentiating Eq. (6) with respect to temperature to get the expression

$$\frac{\partial \ln \gamma_i^1}{\partial T} = \frac{\Delta_{fus}H_i}{RT^2} - \frac{\partial x_i}{x_i \partial T} \tag{7}$$

$\partial x_i/\partial T$ in this expression can be evaluated by taking two points near the eutectic point. The positive values of excess free energy indicate that there is associative interaction between like molecules.

4.4. Microstructure

In general, microstructures (the shape, size of the crystallites) and distribution of phases, play a very significant role in deciding about mechanical, electrical, magnetic and optical properties of materials. The growth morphology [20,21] of a eutectic system is controlled by the growth characteristics of the constituent phases. Depending on interface morphology they can solidify with either faceted or with non-faceted interface. This behaviour is related to the nature of the solid–liquid interface and can be predicted from their entropy of fusion data (Table 1). Hunt and Jackson [6] predicted the structure of the solid–liquid interface of a material in contact with its liquid using interface roughness (α) defined by

$$\alpha = \frac{\xi\,\Delta_{fus}H}{RT} \tag{8}$$

where ξ is a crystallographic factor which is generally equal to or less than one. The values of α are reported in Table 1. If $\alpha > 2$, the interface is quite smooth and the crystal develops with a faceted morphology. On

the other hand if $\alpha < 2$, the interface is rough and many sites are continuously available and the crystal develops with a non-faceted morphology. In the case of the eutectic and monotectic, the situation becomes even more complicated owing to rejection of solute and its subsequent diffusion towards the respective phases.

4.4.1. Microstructure of the monotectic

When a liquid of monotectic composition (Fig. 1) is allowed to cool below the monotectic temperature (T_m), solid DCB deposits. As a result the liquid adjacent to the interface is enriched with SCN owing to solute rejection and becomes supersaturated with respect to SCN; droplets of SCN (L_2) then nucleate to relieve the supersaturation. Whether droplets nucleate in the melt or on the solid–liquid interface, depends on the relative magnitude of the three interfacial energies, namely, σ_{SL_1}, σ_{SL_2} and $\sigma_{L_1L_2}$. The interfacial energy $\sigma_{L_1L_2}$ was calculated using an equation reported earlier [22]. From the data reported in Table 3 it is evident that the Cahn wetting condition could be successfully applied to the present system. Accordingly, the interfacial energies are related by

$$\sigma_{SL_2} < \sigma_{SL_1} + \sigma_{L_1L_2}$$

Thus, the DCB–SCN liquid (L_1) wets the solidified DCB perfectly, and SCN rich droplets (L_2) will be surrounded by DCB–SCN liquid. Under this condition, there is possibility of capillary instability of the type in the Al–Bi system [23]. The unidirectionally solidify optical micrographs of monotectic (Fig. 2(a) and (b)) show the solidification features of monotectic

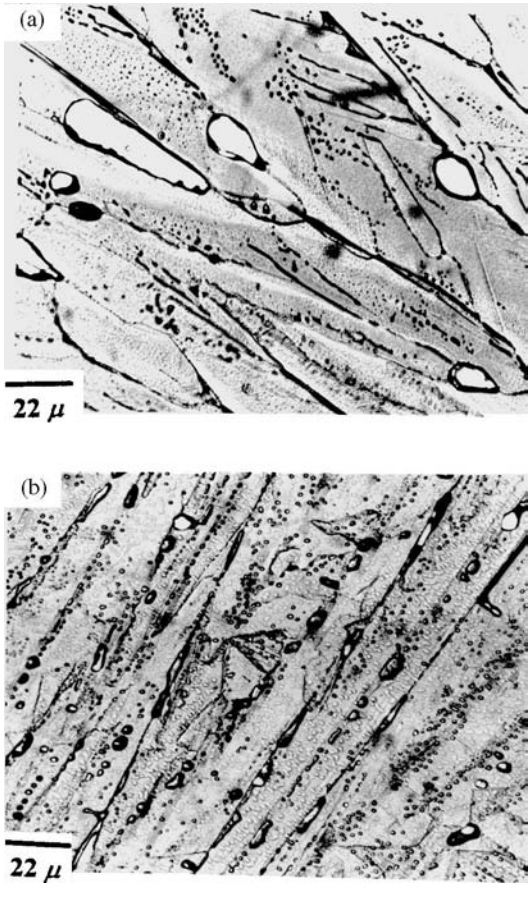

Fig. 2. Optical microphotograph of monotectic: (a) slow rate of solidification; (b) rapid solidification.

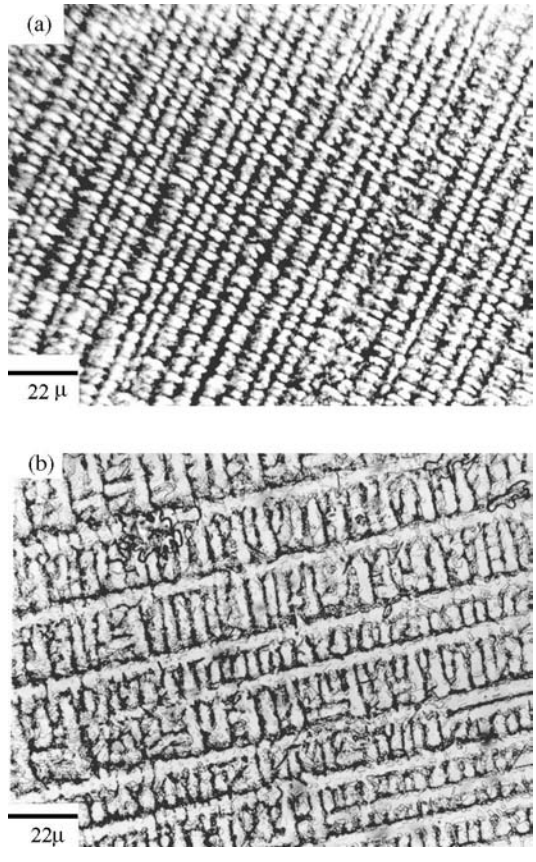

Fig. 3. Optical microphotograph of eutectic: (a) rapid solidification; (b) slow rate of solidification.

alloy. The slow rate solidify microstructure (Fig. 2(a)) shows spherical droplets while rapidly solidified microstructure (Fig. 2(b)) shows elongated spherical shape in a particular direction. In Fig. 2(b) the time for formation of droplets of SCN is longer than the freezing time of DCB, due to this effect SCN droplets are surrounded by the solidified DCB.

4.4.2. Microstructure of the eutectic

The optical micrographs of eutectic (Fig. 3(a) and (b)) show the dendritic structure with primary and secondary arms perpendicular to each other. In the rapid solidify microstructure (Fig. 3(a)) only primary dendritic arms are grown up in a particular direction and secondary arms have no sufficient time to grow. In the second microstructure (Fig. 3(b)), where the solidification rate is slow, the secondary arms have got sufficient time to grow. At few places tertiary arms have also appeared which is due to inhomogeniety in heat distribution during the solidification process.

Acknowledgements

One of the authors Dr. R.N. Rai thanks CSIR, New Delhi, for financial assistance through a Senior Research Fellowship.

References

[1] R. Elliott, Eutectic Solidification Processing, Butterworths, London, 1983.
[2] J. Glazer, Int. Mater. Rev. 40 (1995) 65.
[3] J.B. Andrews, A.C. Sandline, Curreri, Metall. Trans. A 19 (1988) 2651.
[4] K. Rzyman, Z. Moser, R.E. Watson, M. Weinert, J. Phase Equilibria 17 (1996) 173.
[5] R. Trivedi, W. Kurz, Int. Mater. Rev. 32 (1994) 49.
[6] J.D. Hunt, K.A. Jackson, Trans. Met. Soc. AIME 236 (1966) 843.
[7] M.E. Glicksman, N.B. Singh, M. Chopra, Manuf. Space 11 (1982) 267.
[8] V.V. Podolinsky, N.Y. Taran, V.G. Drykin, J. Cryst. Growth 96 (1989) 445.
[9] J.P. Farges, Organic Conductors, Marcel Dekker, New York, 1994.
[10] T. Ishiguro, K. Yamaji, Organic Superconductors, Springer, Berlin, 1990.
[11] Ch. Bosshard, K. Sutter, Ph. Pretre, J. Hulliger, M. Florsheimer, P. Kaatz, P. Gunter, Organic Nonlinear Optical Materials, Gordon and Breach, London, 1995.
[12] N.B. Singh, T. Henningsen, R.H. Hopkins, R. Mazelsky, R.D. Hamacher, E.P. Supertzi, F.K. Hopkins, D.E. Zelmon, O.P. Singh, J. Cryst. Growth 128 (1993) 976.
[13] D.M. Herlach, R.F. Cochrane, I. Egry, H.J. Fecht, A.L. Greer, Int. Mater. Rev. 38 (1993) 273.
[14] B. Derby, J.J. Favier, Acta Metall. 7 (1983) 1123.
[15] A. Ecker, D.O. Frazier, J.I.D. Alexander, Metall. Trans. A 20 (1989) 2517.
[16] U.S. Rai, R.N. Rai, J. Cryst. Growth 191 (1998) 234.
[17] N. Singh, N.B. Singh, U.S. Rai, O.P. Singh, Thermochim. Acta 95 (1985) 291.
[18] J.W. Christian, The Theory of Phase Transformation in Metals and Alloys, Pergamon Press, Oxford, 1965.
[19] U.S. Rai, R.N. Rai, J. Therm. Anal. 53 (1998) 883.
[20] G.A. Chadwick, Metallography of Phase Transformations, Butterworths, London, 1972.
[21] R. Elliot, Int. Mater. Rev. 22 (1997) 161.
[22] U.S. Rai, R.N. Rai, J. Cryst. Growth 169 (1996) 563.
[23] C. Schafer, M.H. Johnston, R.A. Parr, Acta Metall. 31 (1983) 1221.